

Dissolution Kinetics of the Hydrometallurgical Extraction of Tin from a Nigerian Cassiterite Ore Obtained From Jibia Local Government Katsina State

Kehinde Israel Omoniyi*, Zaharaddeen Nasir Garba, Mustapha Yusuf Hamza, Baba Abdullahi Alafara, Aroh Augustina Oyibo and Owolabi Ayowole Awwal

Received: 11 June 2023/Accepted 29 September 2023/Published 04 September 2023

Abstract: *The importance of exploiting mineral resources has grown significantly in developing countries, including Nigeria, as a result of excessive reliance on revenue generated from oil and gas exports and insufficient attention given to exploring solid minerals. This study focused on investigating the leaching kinetics of a Nigerian cassiterite ore in hydrochloric acid. The raw ore and leached residue were subjected to EDXRF analysis to determine chemical composition, SEM imaging to assess morphological structure and photomicrograph, and XRD for mineralogical analysis; The effects of hydrochloric acid concentration, agitation speed, temperature and particle size on the dissolution rates of the ore were examined. The findings revealed that agitation speed, temperature and concentration of hydrochloric acid positively influenced the leaching rate of the cassiterite ore. However, the leaching rate decreased with an increase in particle size. Under optimal leaching conditions (HCl 2.0 mol/L, 75°C, 45 µm, 400 rpm, 120 min.), approximately 87% of the ore reacted within 120 minutes. The reaction order was calculated to be 0.58, while the activation energy was evaluated as 23.72 KJ/mol from the dissolution data. Therefore, the findings find relevance in the design of industrial plants for beneficiation of tin ore; towards boosting sustainable and efficient methods for tin recovery from its ore, and boosting Nigeria's foreign reserves.*

Keywords: Cassiterite ore, hydrochloric acid, leaching, diffusion control

Kehinde Israel Omoniyi^{1*}

Department of Chemistry, Ahmadu Bello University, P.M.B. 06, Zaria-810211, Nigeria

Email: israelflourish@yahoo.com

Orcid id: [0009-005-3224-9382](https://orcid.org/0009-005-3224-9382)

Zaharaddeen Nasir Garba

Department of Chemistry, Ahmadu Bello University, P.M.B. 06, Zaria-810211, Nigeria

Email: dinigetso2000@gmail.com

Mustapha Yusuf Hamza

Department of Chemistry, Ahmadu Bello University, P.M.B. 06, Zaria-810211, Nigeria

Email: myhamza002@gmail.com

Orcid id: <https://orcid.org/0009-0008-6502-6179>

Baba Abdullahi Alafara

Department of Industrial Chemistry, University of Ilorin, P.M.B. 1515, Ilorin, Nigeria

Email: baalafara@yahoo.com

Orcid id: <https://orcid.org/0000-0002-6978-7868>

Aroh Augustina Oyibo

Department of Chemistry, Nigerian Police Academy, Wudil, Kano State, P.M.B. 3474, Kano-713105, Nigeria

Email: augustinaaroh@yahoo.com

Orcid id: <https://orcid.org/0009-0005-2668-2788>

OWOLABI AYOWOLE AWWAL

Department of Chemistry
61455, Western Illinois University, USA

Email: ayowoletune@gmail.com

Orcid id: <https://orcid.org/0000-0001-5258-275X>

1.0 Introduction

Nigeria is blessed with a lot of mineral resources, which have greatly contributed to

the national wealth with associated socio-economic benefits. About 80% of tin mined in Nigeria is from secondary deposits found downstream (tin placer deposits) and derived from primary tin lodes and granitic rocks (Ebikemefa, 2020; Lehmann, 2021). Tin is formed as the primary deposit in the granite rock and at the touching area of metamorphic rock (associated with tourmaline and quartz tin veins), as well as a secondary deposit in it, consisting of alluvium, alluvial, and colluvium sediment (Adiputra *et al.*, 2020).

Cassiterite is the most important tin ore, it occurs in the form of a stannic oxide (SnO_2) with varying colours: black, brown, reddish-brown, or greyish-white is an important ore from which pure tin can be economically extracted (Wang *et al.*, 2022). This colour variation could be due to the presence of iron as the major gangue in combination with other impurities such as tantalum, tungsten, and niobium (Bulatovic and Silvio, 2000).

The purification of concentrates stands as the exclusive industrial implementation of hydrometallurgy within the realm of tin ore and concentrate processing. A pressing demand has arisen for meticulous qualitative and quantitative assessment of various solid minerals found in Nigeria. This serves as an indicator of their prospective industrial and economic applications. Such evaluations are poised to boost the Nigerian economy and establish a methodology for their efficient extraction. This study presents the kinetics of tin extraction through the hydrometallurgical process towards the desire to design economically viable extraction schemes. Hydrothermal extraction has been widely implemented in the extraction of tin from its ore or the recovery or from a leaching residue. For example, Wang *et al.* (2022) adopted the method to recover tin from zinc-leaching residue and obtained a recovered efficiency of 99.8%. The leaching was performed by using 24 g/L of oxalic acid in 0.05 mol/L H_2SO_4 at 60 °C for 30 minutes. Rodlliya *et al.* (2021) also observed 93.2% recovery efficiency from the leaching of zinc from its ore. The leaching was achieved through wet chlorination using HCl. They observed that

the leaching is temperature and time-dependent and also demonstrated that the leaching process can also be achieved without H_2O_2 . Kamberovic *et al.* (2018) developed a successive hydrometallurgical route for the selective recovery of base and precious metals including Sn and recorded efficiency of about 89%. Many studies on the hydrometallurgical recovery of Sn within Nigeria has not been well documented. Since such data can furnish information concerning metallurgy and subsequent application, this study is advocated.

2.0 Materials and Method

2.1 Materials

The cassiterite sample from Jibia Local Government Area Katsina State, Nigeria was obtained from the Ministry of Resource Development, Katsina, Katsina State. The sample was taken selectively, crushed and sieved into three different particle diameters 45, 75, and 100 μm respectively. Distilled water was used in all experiments.

2.2 Leaching procedure

The dissolution experiments were carried out in a 250 ml Pyrex glass reactor, placed in a temperature-controlled water bath set at a given temperature (25°, 40°, 55°, 65°, and 75°C) and a given time (5, 10, 30, 60 and 120 minutes) equipped with a mechanical agitator, and a cooler to avoid loss of solution through evaporation. For each run, 10 g/L of the pulverized ore was added to the solution at a defined lixiviant concentration. The cassiterite ore dissolution rate with HCl solution at different concentrations (0.1mol/L -2.5mol/L) and desired temperature at varied time intervals (5–120 min) was carried out. The lixiviant concentration which gave the maximum dissolution efficiency was used for the optimization of other leaching parameters such as reaction temperature, particle size and agitation speed. The weights of the residue products were measured and the percentage of the dissolved cassiterite ore was calculated using the formula shown in Equation 1



$$\text{Dissolved product (\%)} = \frac{m_i - m_r}{m_i} \times \frac{100}{1} \quad (1)$$

where m_i is the initial mass, m_r is the mass of the residue. The activation energy, E_a and constants were evaluated from the Arrhenius plots. In all cases, the fraction of the cassiterite ore reacted, α , was calculated from the initial difference in weight of the amount reacted or unreacted at various time intervals up to 120 minutes after being oven-dried at about 60 °C. The material purity of the residual product at optimal (75°C and 400rpm in 2.0mol/L HCl) was identified by a powdered X-ray diffractometer (XRD).

3.0 Results and Discussion

3.1 Ore analysis

The elemental chemical analysis by energy-dispersive X-ray fluorescence (EDXRF) analysis using MINI PAL 4 Spectrometer at particle fractions 45 μm shows the presence

of eight major elements, which include 46.94% SnO₂, 20.65% TiO₂, 17.79% Fe₂O₃, 4.95% SiO₂, 2.42% Al₂O₃, 1.56% Ta₂O₅, 1.47 % MnO, and 1.43 % Nb₂O₅. Other compounds detected occurring at low to trace levels included 0.81% CaO, 0.54% P₂O₅, 0.39% ZrO₂, 0.21% K₂O, 0.18% Cl, 0.17% CdO, 0.13% WO₃, 0.10% SO₃, 0.09% Y₂O₃, 0.07% CeO₂.

3.2 Mineralogical analysis

The mineral purity test by X-ray diffraction (XRD) affirmed admixture of Cassiterite (Sn_{2.00}O_{4.00}: 96-900-7434), and ilmenite (Fe_{6.00} Ti_{6.00} O_{18.00}: 96-901-0914) as major compounds present in cassiterite ore before acid treatment (Fig. 1).

Photomicrography revealed, brecciated mineral grains; it contains cryptocrystalline quartz (SiO₂), cassiterite (SnO₂), and tantalite [(Fe, Mn)Ta₂O₆].

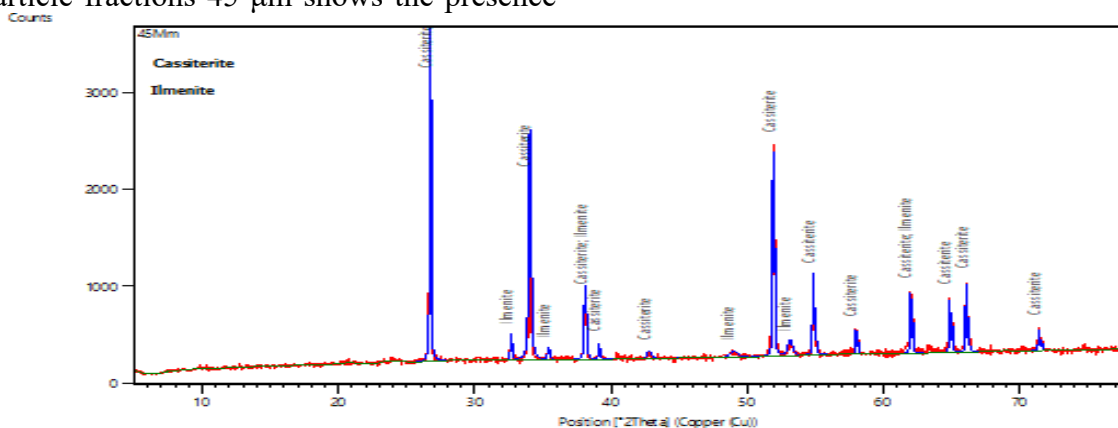


Fig.1 X-Ray diffraction pattern of raw cassiterite ore showing the presence of (1) SnO₂ (cassiterite) {96-900-7434}, (2) FeTiO₃ (siderite) {96-901-0914} as identified with the Joint Committee on Powder Diffraction Standard file number.

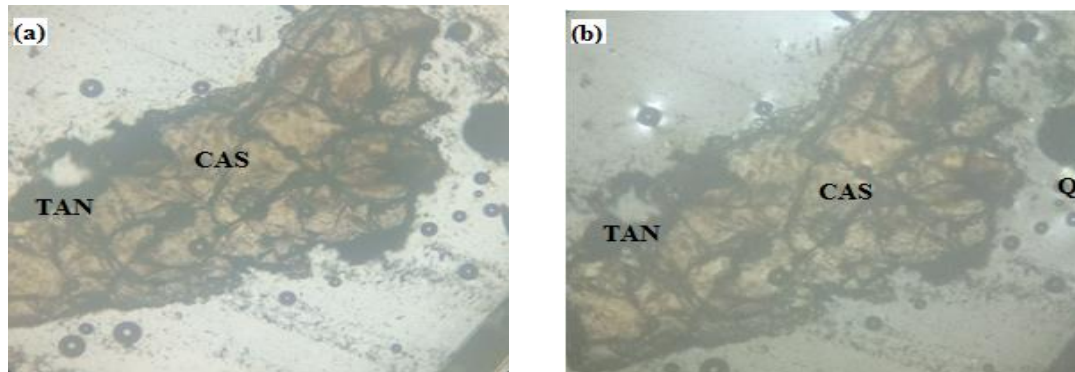


Fig 2: Photomicrograph of Tin ore under (a) Plane polarized light (PPL) and (b) Crossed polarized light (XPL) showing (Q) =Quartz, (CAS) =Cassiterite, and (TAN) =Tantalite, Mag. =X100



3.3 Surface morphology

The surface morphology of the raw cassiterite ore was analysed with scanning electron microscopy leaching. The morphology of the raw cassiterite ore shows agglomerated

particles of various sizes and shapes. The semi-quantitative EDS analysis of the cassiterite ore is mainly composed of 70.05% Sn, 17.25% O, 3.00% C, 2.30% Se, 1.20% Cl, and 6.20% SiO₂.

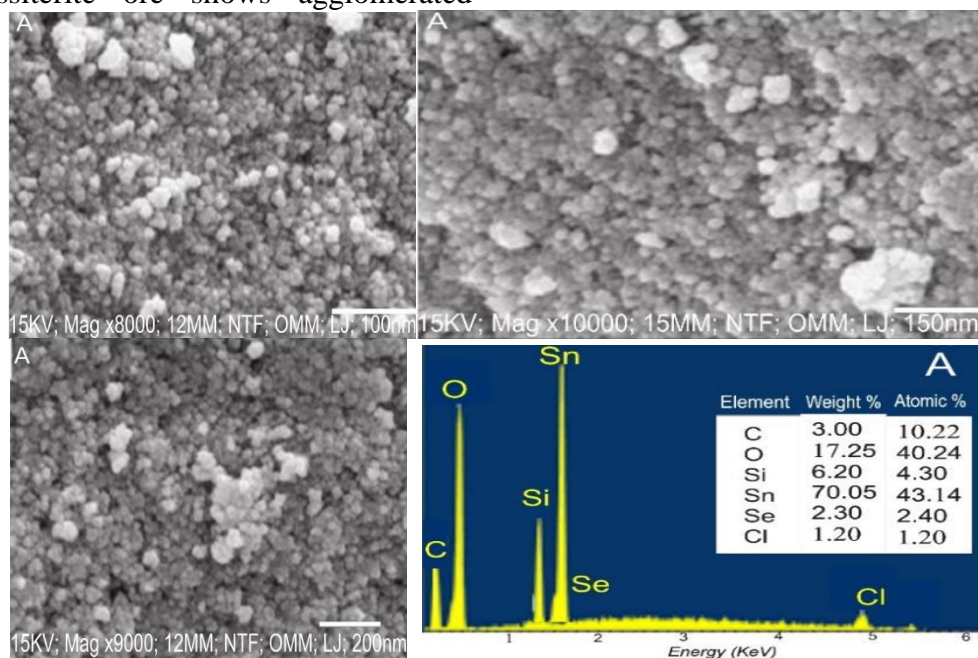


Fig 3 - SEM micrograph of the raw cassiterite ore

3.4 Leaching studies

3.4.1 Effect of variation of HCl concentration

By using 45 μ m particle size at 200 rpm, the effect of HCl concentration (0.1-2.5 mol/L) on the dissolution of the cassiterite ore at 55 °C in 5-120 minutes is presented in Fig. 4. Dissolution of the cassiterite was highest by using 2.0 mol/L HCl concentration. Increasing the lixiviant (HCl) concentration appreciably increased the ore dissolution using 0.1 mol/L HCl solution up to 2.0 mol/L. By using 0.1 mol/L HCl, 26% of the ore reacted, while 57% reacted with 2.0 mol/L HCl solution within 120 min. Additionally, when the concentration of hydrochloric acid was increased to 2.5 mol/L, the ore dissolution decreased, reaching 54% after 120 minutes. This could be related to the precipitation phenomenon at higher lixiviant concentrations, as described by Baba *et al.*, (2020).

The associated compounds in the cassiterite become more stable and require high energy to dissolve (Lalasari *et al.*, 2020). So, the

cassiterite (SnO₂) dissolves in HCl solutions by forming a stable H₂(SnCl₆) complex. Therefore, the possible dissolution reaction of cassiterite ore by hydrochloric solution is consistent with the following stoichiometry:

$$\text{SnO}_{2(s)} + 6\text{HCl}_{(aq)} \rightarrow \text{H}_2(\text{SnCl}_6)_{(aq)} + 2\text{H}_2\text{O}_{(aq)}$$

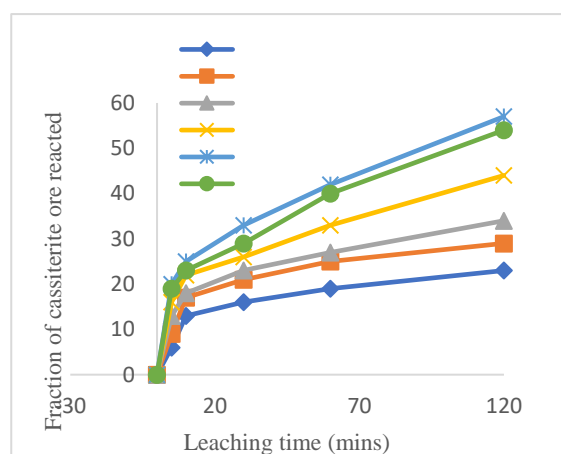


Fig.4 Effect of [HCl] on the dissolution of cassiterite at different leaching times

Experimental conditions: [HCl] = 0.1–2.5 mol/L, reaction temperature = 55 °C, particle size = 45 μ m, solid-to-liquid ratio = 10 g/L



3.4.2 Influence of Agitation Speed

At 75 °C and various time intervals (5-150 min) in 2.0 mol/L HCl with 45 μm particle size, the effect of agitation speed (100–600 rpm) on the dissolution of tin ore evaluated is depicted in Fig. 5. Agitation establishes a homogeneous suspension that allows for effective mass transfer of the reactants. Tin dissolution increases slightly from 5 to 120 minutes as agitation speed increases from 100–600 rpm. The leaching reached optimum condition at 400 rpm, reducing the influence of liquid film boundary diffusion. Further, a minor decrease was observed when the agitation speed was set to 500 and 600 rpm. This could be linked to the instabilities of the cassiterite ore's contact area (Regna and Yusdianto, 2020).

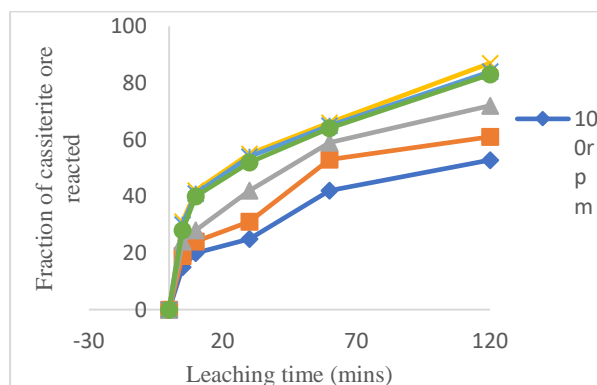


Fig.5 Effect of Agitation speed on the dissolution of cassiterite at different leaching times (Experimental conditions: [HCl] 2.0mol/L Agitation speed= 100–600 rpm, reaction temperature = 75 °C, particle size = 45 μm, solid-to-liquid ratio = 10 g/L)

3.4.3 Effect of variation of temperature

From Fig. 6, at the optimum concentration of 2.0 mol/L HCl, 45μm particle size and 400 rpm, the impact of temperature (25 to 75 °C) at leaching time of 5-120 min indicated that the dissolution rate of tin increases with increase in temperature.

The dissolution rate of tin after 120 minutes reaches 18% and 87% at 25 and 75 °C, respectively. The dissolution rate is larger at 75 °C due to the acceleration of the mass transfer coefficient and diffusivity at higher temperatures, which improves the tin leaching rates (Lee *et al.*, 2015).

This is consistent with the idea that when a substance is heated, particles acquire more kinetic energy and collide more frequently, accelerating the rate of reaction (Liu *et al.*, 2010; Baba *et al.*, 2017).

3.4.4 Effect of variation of particle size

From Fig. 7, by using the particle sizes (45 μm 75μm and 100μm), 2.0mol/L HCl solution at 75 °C and 400 rpm; at 2.0 mol/L HCl and 120 minutes 68%, 75%, and 87% of the ore reacted with particle sizes of 100, 75 and 45μm respectively. Variations in particle size can have a significant impact on the efficiency of tin ore dissolution.

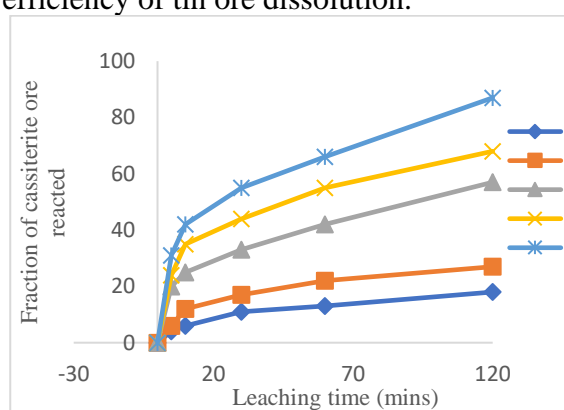


Fig. 6 Effect of temperature on the dissolution of cassiterite in HCl leaching (Experimental conditions: [HCl] = 2.0 mol/L, Agitation speed = 400rpm, reaction temperature = 25–75 °C, particle size = 45 μm, solid to-liquid = 10 g/L)

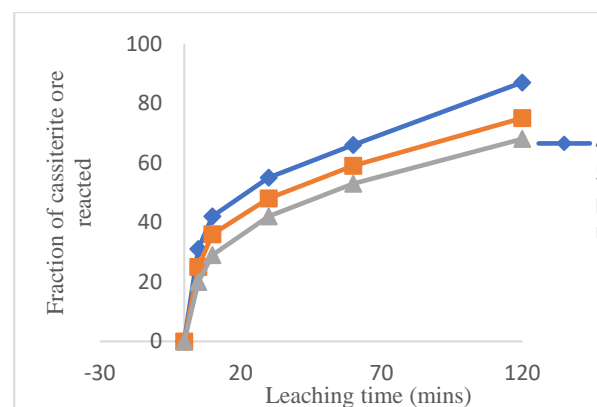


Fig.7 Effect of particle size on the dissolution rate of cassiterite ore (Experimental conditions: [HCl] = 2.0 mol/L, Agitation speed= 400rpm, reaction temperature = 75 °C, solid-to-liquid = 10 g/L)



3.5 Dissolution kinetics analysis

The unreacted-core model can be used for kinetics calculations because insoluble gangue minerals covering the unreacted cassiterite surface form an ash layer. However, the rate-determining step may be one of the following three steps: (1) diffusion through the liquid film surrounding solid particles; (2) diffusion through the ash/inert solid layer; and (3) chemical reaction on the unreacted core surface. The simplified equations of the shrinking core model when liquid film diffusion, ash/inert solid layer diffusion, or the surface chemical reactions is the slowest step can be expressed by stoichiometries as summarized (Raji *et al.*, 2020):

For a surface chemical reaction controlled process, the equation that applies is:

$$1 - (1 - \alpha_B)^{1/3} = k_1 t \quad (2)$$

where $k_1 = \frac{bkC_{Ab}}{PR}$, k is the reaction rate (ms^{-1}), C_{Ab} is the concentration of A in the bulk of the fluid (mol/m^3), P is the molar density of B (mol/m^3), R is the radius of the solid particle (m), t is time (s), and α_B is the fraction of B reacted.

For an internal diffusion-controlled process, the equation that applies is:

For a surface chemical reaction controlled process, the equation that applies is:

$$1 - \frac{2}{3}\alpha_B - (1 - \alpha_B)^{2/3} = k_2 t \quad (2)$$

where $k_2 = \frac{6bD_oC_{Ab}}{PR^2}$, D_o is the effective diffusion coefficient of A through the product layer (m^2s^{-1}) For a mixed controlled process, the following equation holds:

$$1 - (1 - \alpha_B) + \frac{1}{6} \left[(1 - \alpha_B)^{1/3} + 1 - 2(1 - \alpha_B)^{2/3} \right] = k_3 t \quad (3)$$

To determine the most fitted controlling mechanisms during tin ore dissolution, Sn-concentration data in the suggested equations (1 – 3) were employed in the treatments of the dissolution kinetic data results obtained. Consequently, the experimental data obtained from Fig 4 and 5 were appropriately subjected to equations (1 – 3) to determine the reaction order and activation energy for kinetic assessment through relevant Arrhenius plots. During the preliminary trials with the two appropriate models, it was found that only the shrinking core model equation (2) fitted perfectly into the dissolution data with the average correlation of $R^2 = 0.9851 > R^2 = 0.628, 0.7997$ by using equations (1) and (3) models respectively.

Hence, in this investigation, the diffusion equation model (2) was used subsequently in the treatment of dissolution results.

For example, the dissolution data in Fig 4 were treated with equation (2) to obtain Fig 7.

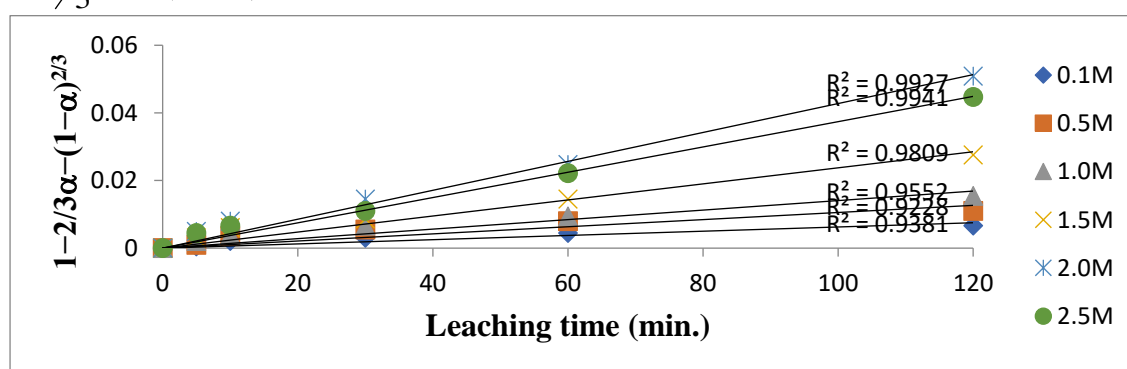


Fig. 8: Plot of $1 - \frac{2}{3}\alpha - (1 - \alpha)^{2/3}$ vs. leaching time (min.) at different HCl concentrations

The experimental rate constants, k_1 , were determined from the slopes in Fig 7 and the plots of $\ln k_1$ vs. $\ln [\text{HCl}]$ were made as shown in Fig 9.

The slope of the resulting plot (Fig 9) indicates that the reaction order is $0.5892 \approx 1$

with respect to H^+ ion, for HCl concentration ≤ 2.5 M. Also, Fig 6 was linearized with the relation $1 - \frac{2}{3}\alpha - (1 - \alpha)^{2/3}$ versus time at different temperatures, as shown in Fig 10.



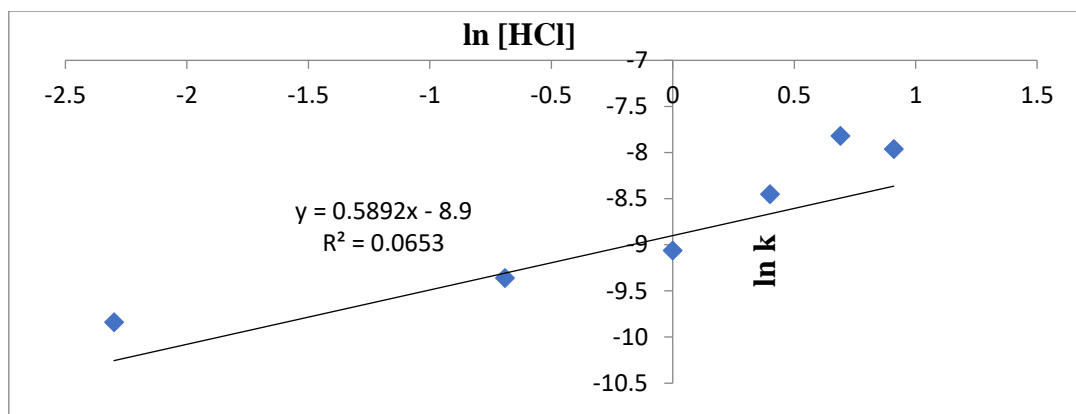


Fig. 9: Plot of $\ln k_1$ vs. $\ln [\text{HCl}]$

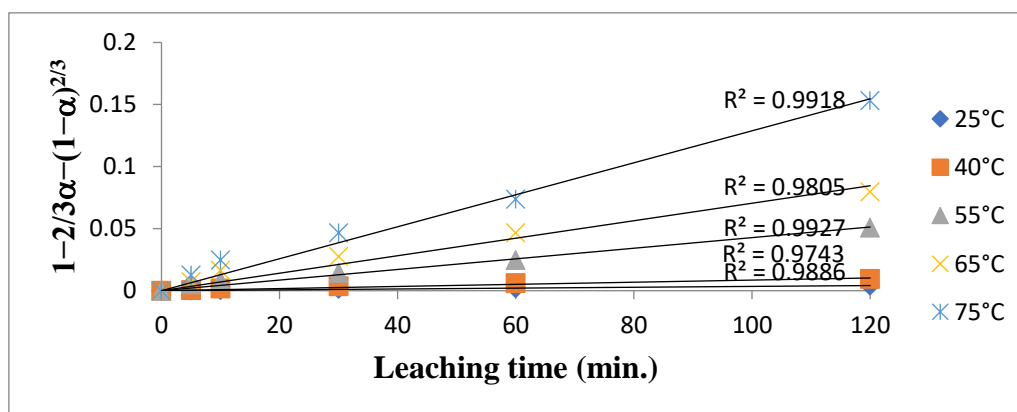


Fig. 10: Plot of $1 - \frac{2}{3}\alpha - (1 - \alpha)^{\frac{2}{3}}$ versus leaching time (min.) at different temperatures

According to Baba *et al.* (2017), diffusion-controlled heterogeneous reactions are modestly temperature-dependent, whereas chemically controlled processes are substantially temperature-dependent. The activation energy of a diffusion-controlled process is often less than 40 kJ/mol, whereas the activation energy of a chemically controlled reaction is typically larger than 40 kJ/mol. As a result, the activation energy of a leaching reaction can be utilized to forecast the process's rate-controlling step. Also, the temperature dependence of the specific rate constant can be estimated from the Arrhenius expression:

$$k = A e^{-E_a/RT} \quad (4)$$

A is the frequency factor; k is the specific rate constant; E_a is the activation energy (Jmol^{-1}); R is the universal gas constant ($8.314 \text{ Jmol}^{-1}\text{K}^{-1}$) and T is the absolute temperature.

The result of XRD analysis relating to the leached residue is presented in Fig. 12. From Fig. 12, the peaks of SnO_2 (cassiterite) disappeared when compared to the XRD

(K). Hence, equation (4) was linearized to obtain equation (5):

$$\ln k = \ln A - \frac{E_a}{RT} \quad (5)$$

The activation energy for the process of transforming the sample from the solid phase into solution can represent the basic phenomenon behind the kinetics of tin ore dissolution in HCl solution. The activation energy, E_a , estimated from the slope of Fig 11 for the dissolution process was 23.72 kJ/mol, indicating the diffusion-controlled reaction mechanism as the rate-determining step (Baba *et al.*, 2020; Xuin *et al.*, 1986).

Also, the positive value of 23.72 kJ/mol indicates that tin ore dissolving in HCl solution is favoured by increasing temperature, agitation speed, hydrogen ion concentration, and decreasing particle size.

3.6 Residual product analysis

spectral in Fig. 1. This result shows that the cassiterite ore had been leached by using hydrochloric acid as lixivant. The SEM images of the leached residues with a



diameter of 45 μm at 75 °C by 2.0 mol/L HCl are presented in Fig. 13. The morphology of the leached cassiterite ore reveals a nodular shape whisker with an oval shape. Hence, the

EDS pattern as shown in Fig. 11 gave C (5.2 wt%), O (5.3 wt%), Fe (11.2 wt%), K (25.2 wt%), and Si (33.17 wt%) respective

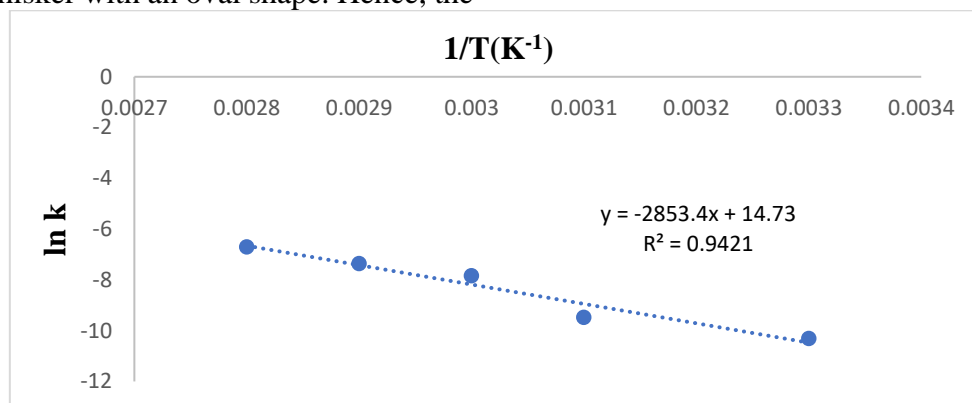


Fig. 11: A plot of ln k versus 1/T(K⁻¹).

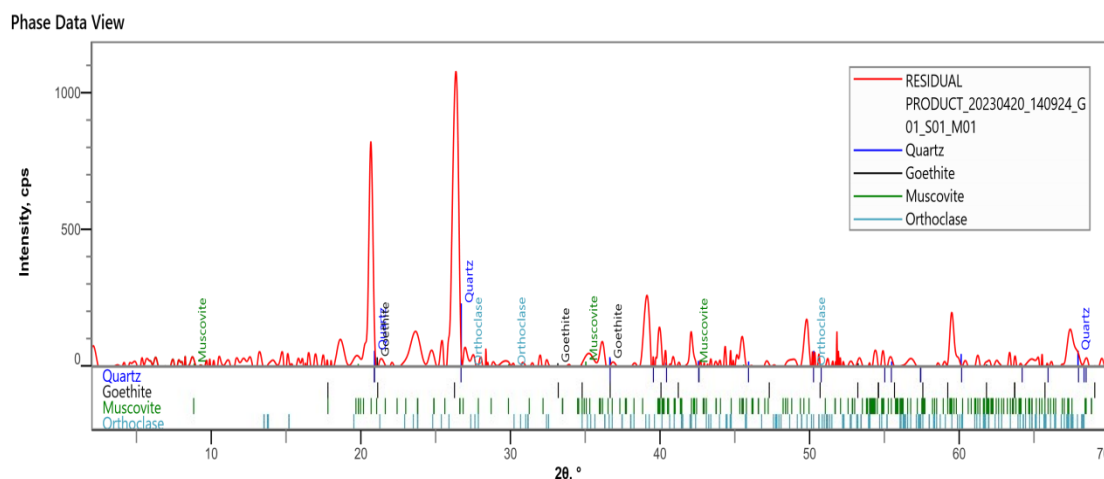


Fig. 12 X-ray diffraction spectrum of the leached product at optimal leaching conditions

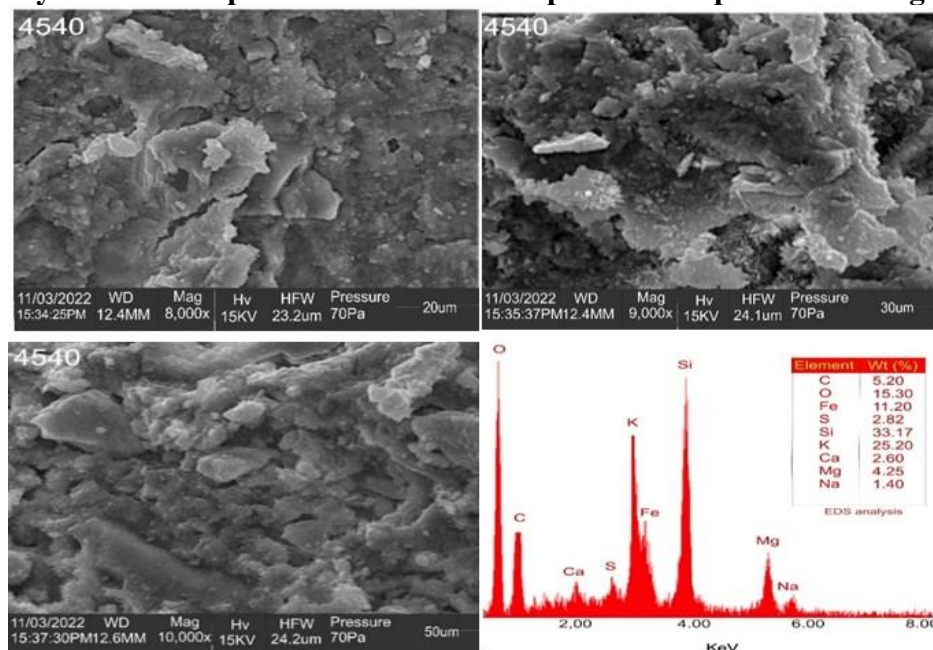


Fig 13: SEM images of leached HCl product of the cassiterite ore at optimal conditions (HCl = 2.0 mol/L, 75 °C, 45 μm, 400rpm, 120 min.)



4.0 Conclusion

The elemental analysis of the ore by X-ray fluorescence (XRF) showed that the cassiterite mineral used in this study contains 46.94% SnO₂, 20.65% TiO₂, 17.79% Fe₂O₃, 4.95% SiO₂, 2.42% Al₂O₃, 1.56% Ta₂O₅, 1.47% MnO, 1.43% Nb₂O₅. Other compounds detected occurring at low to trace levels include 0.81% CaO, 0.54% P₂O₅, 0.39% ZrO₂, 0.21% K₂O, 0.18% Cl, 0.17% CdO, 0.13% WO₃, 0.10% SO₃, 0.09% Y₂O₃, 0.07% CeO₂. The XRD analysis confirmed the originality of cassiterite (Sn_{2.00}O_{4.00}: 96-900-7434), and ilmenite (Fe_{6.00} Ti_{6.00} O_{18.00}: 96-901-0914) as major compounds present in cassiterite ore.

The dissolution rate of tin had the optimal conditions: 2.0 mol/L HCl, 45 µm particle size, 75°C reaction temperature, and 400 rpm agitation speed, yielding approximately 87% tin within 120 minutes.

The dissolution of the cassiterite is controlled by diffusion kinetics. The activation energy was 23.72 kJ/mole and the reaction order concerning the concentrations of hydrochloric acid is 0.58. EDS and phase analyses of the residues provided evidence that cassiterite was completely dissolved in hydrochloric acid under optimal conditions. Therefore, these findings contribute to better understanding the leaching behaviour of cassiterite ore in hydrochloric acid; providing insights for the development of efficient extraction processes in the mining industry.

5.0 References

- Adiputra R N, Agustin F, Sulastri A, Abdullah C I, Nugraha I, Andriansyah R & Hadiprayitno M (2020). The tin ore separation process and optimizing the rare earth mineral (monazite) as a by-product of tin mining in East Belitung Regency. IOP Conference Series: Earth and Environmental Science *IOP Conf. Ser.: Earth Environ. Sci.* 413 012004.
- Baba, A. A., Kayode, J. O. & Raji, M.A. (2020). Low-Energy Feasibility for Leaching an Indigenous Scheelite Ore for Industrial Applications. *Journal of Sustainable Metallurgy*, 6, pp. 659 – 666.
- Baba, A A., Balogun, F., Olaoluwa, T., Bale, B., Adekola, A. and Alabi, F. (2017). Leaching kinetics of a Nigerian complex covellite ore by the ammonia-ammonium sulfate solution. *Korean Journal of Chemical Engineering*, 0256-1115, doi.org/10.1007/s11814-017-0005-5
- Bulatovic S, De Silvio E (2000) Process development for impurity removal from a tin gravity concentrate. *Miner Eng.*, 13, 8-9, pp. 871-879.
- Houchin MR (1985) Surface titrations and electrokinetic measurements on Australian cassiterites. *Colloids Surf* 16:117–126., [doi.org/10.1016/0166-6622\(85\)80246-8](https://doi.org/10.1016/0166-6622(85)80246-8)
- Imeokparia E. G. (2015) *The Applied Geochemist and the challenges of georesource evaluation for sustainable development and environmental management*. Inaugural Lecture delivered at University of Benin, Benin City, Edo State, Nigeria.
- Lalasari, L. H. (2020) Kelarutan mineral ikutan kasiterit dalam asam klorida encer (HCl 10 %) menggunakan reaktor yang dilengkapi pengaduk *J. Tek. Mesin Cakram* 3 97, doi.org/10.32493/jtc.v3i2.7558
- Lee, S., Yoo, K., Kumar, M. & Lee, J. (2015). Separation of Sn from waste Pb-Free Sn—Ag—Cu solder in hydrochloric acid solution with ferric chloride. *Hydrometallurgy*, 157, pp. 184–187, <https://doi.org/10.1016/j.hydromet.2015.08.016>
- Levenspiel O., (1972). *Chemical Reaction Engineering*, Wiley, New York, 361.
- Liu W., Tang M. T., Tang C. B., He J., Yang, S. H. & Yang J. G., (2010) solid-state interfacial reactions in electrodeposited Cu/Sn couples. *Trans. Nonferrous Met. Soc. China*, 20, 910. [https://doi.org/10.1016/s1003-6326\(09\)60102-3](https://doi.org/10.1016/s1003-6326(09)60102-3)
- Raji, M. A., Baba, A. A., Bale, R. B., Alabi, A. G. F. & Ghosh, M. K. (2020). Removal of iron impurities from a Nigerian Biotite-rich Kaolinite ore by a Sulphuric acid solution. *Journal of Chemical*



- Technology and Metallurgy*, 55, 6, pp. 2128 -2135.
- Regna Tri Jayanti & Yusdianto (2020). *Effect of Agitation speed and leaching Time for Nickel recovery of morowali liumonite Ore in Atmospheric Citric Acid Leaching*. Proceedings of 2nd faculty of industrial Technology international congress Bandung, Indonesia, January 28-30, 2020.
- Xuin, G. H., Yu, D. Y. & Su, Y. F. (1986). Leaching of scheelite by hydrochloric acid in the presence of phosphate. *Hydrometallurgy*, 16, 1, pp. 27-40.
- Rodllyah, I., Wijayanti, R., Septiarant, A., Sudrajat, A. & Firmansyah, D. (2021). The extraction of tin (Sn) from primary tin ore deposits using wet chlorination. *IOP Conference Series Earth and Environmental Science*, 882, 1, 012007, DOI: [10.1088/1755-1315/882/1/012007](https://doi.org/10.1088/1755-1315/882/1/012007).
- Kamberović, Ž., Ranitović, M., Korać, M., Andjić, Z., Gajić, N., Djokić, J. & Jevtić, S. (2018), Hydrometallurgical process for selective metals recovery from waste-printed circuit boards. *Metals*, 8, 441. <https://doi.org/10.3390/met8060441>
- Lehmann, B. (2021). Formation of tin ore deposits: A reassessment. *Lithos*, 402-403, <https://doi.org/10.1016/j.lithos.2020.105756>.
- Ebikemefa, C. E. (2020). Benefits of cassiterite mining by artisanal miners in Jos Plateau, Nigeria. *Bull Natl Res Cent.*, 44, 13, <https://doi.org/10.1186/s42269-020-00373-1>.
- Wang, Y., Liu, B., Sun, H., Huang, Y. & Han, G. (2022). Selective extraction and recovery of tin from hazardous zinc-leaching residue by oxalic acid/sulfuric acid mixture leaching and hydrolytic precipitation. *Journal of Cleaner Production*, 342, <https://doi.org/10.1016/j.jclepro.2022.130955>.

Declarations

The authors declare that they have no conflict of interest.

Data availability

All data used in this study will be readily available to the public.

Consent for publication

Not Applicable.

Availability of data and materials

The publisher has the right to make the data public.

Competing interests

The authors declared no conflict of interest.

Funding

There is no source of external funding.

Authors' contribution

Mustapha Yusuf Hamza conducted the research, with Kehinde Israel Omoniyi, Zaharadden Nasir Garba, and Baba Abdullahi Alafara serving as members of the supervisory team. Aroh Augustina Oyibo and Owolabi Ayowole Awwal also contributed by assisting with data analysis and providing access to the necessary equipment at a rebate.

